PERGAMON

International Journal of Solids and Structures 36 (1999) 4991–5012

INTERNATIONAL JOURNAL OF SOLIDS and STRUCTURES

www.elsevier.com/locate/ijsolstr

A homogenization theory for time-dependent nonlinear composites with periodic internal structures

X. Wu[1], N. Ohno*

Department of Mechanical Engineering, Nagoya University, Chikusa-ku, Nagoya 464–8603, Japan

Received 20 September 1997; in revised form 23 July 1998; accepted 2 August 1998

Abstract

A homogenization theory for time-dependent deformation such as creep and viscoplasticity of nonlinear composites with periodic internal structures is developed. To begin with, in the macroscopically uniform case, a rate-type macroscopic constitutive relation between stress and strain and an evolution equation of microscopic stress are derived by introducing two kinds of Y-periodic functions, which are determined by solving two unit cell problems. Then, the macroscopically nonuniform case is discussed in an incremental form using the two-scale asymptotic expansion of field variables. The resulting equations are shown to be effective for computing incrementally the time-dependent deformation for which the history of either macroscopic stress or macroscopic strain is prescribed. As an application of the theory, transverse creep of metal matrix composites reinforced undirectionally with continuous fibers is analyzed numerically to discuss the effect of fiber arrays on the anisotropy in such creep.

1. Introduction

The homogenization method based on the two-scale asymptotic expansion of field variables was developed for composites with periodic or quasi-periodic internal structures (Bensoussan et al., 1978; Sanchez-Palencia, 1980; Bakhvalov and Panasenko, 1989; Kalamkarov, 1992). This method is effective for evaluating both macroscopic constitutive equations and microscopic distributions of stress and strain in such composites.

The homogenization method mentioned above has been employed successfully to solve not only elastic but also elastoplastic problems. For example the method was applied to dynamics of laminated elastic media (Murakami et al., 1981), elasticity with interfacial slip at interface (Lene and Leguillon, 1982), and linear thermoelasticity (Ene, 1983; Francfort, 1983). Implementation of

* Corresponding author. Fax: 81 52 789 5131; e-mail: ohno@mech.nagoya-u.ac.jp

[1] Currently at Rock Engineering Department, OYO Corporation, 2-61-5 Toro-cho, Omiya, Saitama 330-8632, Japan.

0020-7683/99/$ - see front matter
PII: S0020-7683(98)00236-4

the method in adaptive finite element analysis was described by Guedes and Kikuchi (1990). Homogenized constitutive equations of plasticity with internal variables were discussed in conjunction of the method by Suquet (1983, 1985). Moreover, the method has been used for analyzing nonlinear wave propagation (Murakami et al., 1992), elastoplastic constitutive properties of a unit cell (Jansson, 1992), finite elastoplastic deformation of composites (Agah-Tehrani, 1990; Terada et al., 1995), fracture of woven fabric composites (Takano and Zako, 1995), and so on.

For time-dependent deformation, on the other hand, the homogenization method was applied only to linear viscoelasticity and steady-state creep. Linear viscoelasticity can be dealt with in the same manner as in elasticity, since the Laplace transformation allows the governing equations of linear viscoelasticity to be reduced in effect to those of elasticity. Use of the homogenization method in this approach to linear viscoelasticity was described by Sanchez-Palencia (1980) and Shibuya (1996). Linear thermoviscoelasticity of periodic composites was discussed rigorously on the basis of the homogenization method by Francfort and Suquet (1986). The steady-state in creep in structures can be analyzed in general by solving the analogous problem which is established by replacing steady-state creep rate with plastic strain (Hoff, 1954). Hence, the homogenization method extended for nonlinear elasticity (e.g., Jansson, 1992) is applicable to analyzing the steady-state creep behavior of unit cells with periodic boundary conditions. In fact, to verify a constitutive model of steady-state creep of fiber-reinforced composites, Aravas et al. (1995) solved numerically the analogous problem of unit cells on which the requirements of the homogenization method were imposed.

The homogenization method based on the asymptotic expansion has an advantage that the microscopic, as well as the macroscopic, stress and strain states in composites can be analyzed. The method is thus in contrast to simple models effective for the overall behavior of composites. Li and Weng (1997) proposed such a simple model for time-dependent deformation of composites by introducing a linear viscoelastic comparison composite with secant viscosity. Fotiu and Nemat-Nasser (1996), on the other hand, developed a numerical method to compute the overall behavior of elastic–viscoplastic periodic composites by expressing the variables in Fourier series to satisfy the periodic condition.

This paper describes a homogenization theory for time-dependent deformation such as creep and viscoplasticity of nonlinear composites with periodic internal structures within the framework of infinitesimal strain. The theory is developed first in the macroscopically uniform case in a rate form without recourse to the asymptotic expansion, and then it is extended to the macroscopically nonuniform case in an incremental form using the asymptotic expansion. Thus a macroscopic constitutive equation and a microscopic stress evolution equation are derived in rate and incremental forms by introducing two kinds of Y-periodic functions, which are determined by solving two unit cell problems. As an application of the theory, transverse creep of metal matrix composites reinforced unidirectionally with continuous fibers is analyzed numerically by solving the unit cell problems discretized with finite elements, so that the effect of fiber arrays on the anisotropy in the transverse creep is discussed.

2. Homogenization in macroscopically uniform case

To begin with, let us consider a simple case in which a body Ω with a periodic internal structure consisting of at least two constituents is subjected to macroscopically uniform strain and stress.

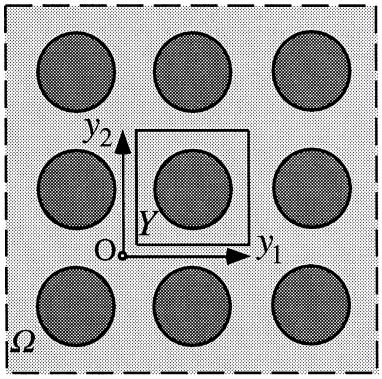

Fig. 1. Periodic composite and representative unit cell.

The homogenized behavior of Ω then can be discussed by analyzing the smallest repeatable element, i.e., unit cell Y, shown in Fig. 1. Only infinitesimal strain is assumed to take place in Y.

2.1. Basic equations

Let us denote the distributions of stress and strain in the cell as $\sigma_{ij}(\boldsymbol{y}, t)$ and $e_{ij}(\boldsymbol{y}, t)$, respectively, where y_i $(i = 1, 2, 3)$ are the local rectangular coordinates taken for the unit cell Y, and t indicates time. From now on σ_{ij} and e_{ij} will be referred to as micro-stress and micro-strain, respectively. Equilibrium of micro-stress can be expressed in a rate form

$$\frac{\partial \dot{\sigma}_{ij}}{\partial y_j} = 0, \tag{1}$$

where the superposed dot denotes the differentiation with respect to time t.

The constituents of Ω are assumed to exhibit linear elasticity and nonlinear creep characterized by

$$\dot{\sigma}_{ij} = c_{ijkl}[\dot{e}_{kl} - \beta_{kl}(\boldsymbol{\sigma})], \tag{2}$$

where c_{ijkl} and β_{kl} indicate, respectively, the elastic constants and creep functions of the constituents, and they satisfy

$$c_{ijkl} = c_{jikl} = c_{ijlk} = c_{klij}, \tag{3}$$

$$\beta_{kl} = \beta_{lk}. \tag{4}$$

Hereafter c_{ijkl} and β_{kl}, which can vary from constituent to constituent, will be regarded as functions of the local coordinates y_i though not expressed explicitly.

The microscopic velocity field $\dot{u}_i(\boldsymbol{y}, t)$ in Y in the case of macroscopically uniform deformation has the following expression if H_{ij} denotes the gradient of macroscopic displacement:

$$\dot{u}_i(\boldsymbol{y}, t) = \dot{H}_{ij}(t) y_j + \dot{u}_i^1(\boldsymbol{y}, t). \tag{5}$$

Then micro-strain rate $\dot{e}_{ij}$ in eqn (2) is expressed as

$$\dot{e}_{ij} = \dot{E}_{ij} + e_{ij(y)}(\dot{\boldsymbol{u}}^1), \tag{6}$$

where $\dot{E}_{ij}$ and $e_{ij(y)}(\dot{\boldsymbol{u}}^1)$ denote macro-strain rate and perturbed strain rate, respectively:

$$\dot{E}_{ij} = \tfrac{1}{2}(\dot{H}_{ij} + \dot{H}_{ji}), \tag{7}$$

$$e_{ij(y)}(\dot{\boldsymbol{u}}^1) = \frac{1}{2}\left(\frac{\partial \dot{u}_i^1}{\partial y_j} + \frac{\partial \dot{u}_j^1}{\partial y_i}\right). \tag{8}$$

Since $\dot{u}_i^1$ represents the perturbation of microscopic velocity $\dot{u}_i$ from macroscopic one $\dot{H}_{ij}y_j$, $\dot{u}_i^1$ satisfies the periodic condition resulting from the periodic internal structure. Hence, when $\dot{u}_i^1$ is to be found, $\dot{u}_i^1$ is required to be a function satisfying this periodic condition. Such a function is called Y-periodic.

2.2. Solution for perturbed velocity field

Now, on the supposition that the current distribution of micro-stress in Y, $\sigma_{ij}(\boldsymbol{y}, t)$, is known, we find the current field of perturbed velocity in Y, $\dot{u}_i^1(\boldsymbol{y}, t)$, which is Y-periodic and satisfies eqns (1), (2) and (6).

Let $v_i(\boldsymbol{y}, t)$ be an arbitrary, Y-periodic velocity field defined in Y at t. Then, the use of the integration by parts and the divergence theorem allows eqn (1) to be transformed to

$$\int_Y \dot{\sigma}_{ij} e_{ij(y)}(\boldsymbol{v})\,\mathrm{d}Y - \int_S \dot{\sigma}_{ij} n_j v_i\,\mathrm{d}S = 0, \tag{9}$$

where S denotes the boundary of Y, and n_i indicates the unit vector outward to S. The second term in the above equation vanishes because $\dot{\sigma}_{ij}$ and v_i are Y-periodic and n_i takes opposite directions on opposite boundary surfaces of Y. Hence eqn (9) becomes

$$\int_Y \dot{\sigma}_{ij} e_{ij(y)}(\boldsymbol{v})\,\mathrm{d}Y = 0. \tag{10}$$

Since $v_i(\boldsymbol{y}, t)$ is considered to be a virtual field of $\dot{u}_i^1$, the above equation can be interpreted as a rate form of the principle of virtual work pertinent to unit cells of periodic composites. Substitution of eqns (2) and (6) into eqn (10) results in

$$\int_Y c_{ijpq} e_{pq(y)}(\dot{\boldsymbol{u}}^1) e_{ij(y)}(\boldsymbol{v})\,\mathrm{d}Y = -\dot{E}_{kl}\int_Y c_{ijkl} e_{ij(y)}(\boldsymbol{v})\,\mathrm{d}Y + \int_Y c_{ijkl}\beta_{kl}(\boldsymbol{\sigma}) e_{ij(y)}(\boldsymbol{v})\,\mathrm{d}Y. \tag{11}$$

Consequently, the problem to find $\dot{u}_i^1(\boldsymbol{y}, t)$ is restated as follows: on the supposition that the current distribution of micro-stress in Y, $\sigma_{ij}(\boldsymbol{y}, t)$, is known, we find the current field of perturbed velocity in Y, $\dot{u}_i^1(\boldsymbol{y}, t)$, which is Y-periodic and satisfies eqn (11) for any Y-periodic velocity field $v_i(\boldsymbol{y}, t)$ defined in Y at t.

Now let χ_i^{kl} and φ_i be the functions which are determined by solving the following boundary value problems for the unit cell Y, respectively:

$$\int_Y c_{ijpq} e_{pq(y)}(\boldsymbol{\chi}^{kl}) e_{ij(y)}(\boldsymbol{v})\,\mathrm{d}Y = \int_Y c_{ijkl} e_{ij(y)}(\boldsymbol{v})\,\mathrm{d}Y \quad \text{with } Y\text{-periodicity of } \boldsymbol{\chi}_i^{kl}, \tag{12}$$

$$\int_Y c_{ijpq} e_{pq(y)}(\boldsymbol{\varphi}) e_{ij(y)}(\boldsymbol{v})\,\mathrm{d}Y = \int_Y c_{ijkl} \beta_{kl}(\boldsymbol{\sigma}) e_{ij(y)}(\boldsymbol{v})\,\mathrm{d}Y \quad \text{with } Y\text{-periodicity of } \varphi_i, \tag{13}$$

where $v_i(\boldsymbol{y}, t)$ is any Y-periodic velocity field in Y at t. Then eqn (11), in which $\dot{u}_i^1$ depends linearly on $\dot{E}_{kl}$ through the first term in the right hand side, has a solution

$$\dot{u}_i^1(\boldsymbol{y}, t) = -\chi_i^{kl}(\boldsymbol{y})\dot{E}_{kl}(t) + \varphi_i(\boldsymbol{y}, t). \tag{14}$$

It is noticed that χ_i^{kl} is a function of only y_j because χ_i^{kl} results from the distribution of c_{pqrs} in Y, as seen from eqn (12). This is in contrast to $\varphi_i(\boldsymbol{y}, t)$ defined by eqn (13), in which $c_{pqrs}\beta_{rs}(\boldsymbol{\sigma})$ is a function of y_j and t because of $\sigma_{ij}(\boldsymbol{y}, t)$. It is also noticed that eqns (12) and (13) are not reduced identically to $e_{pq(y)}(\boldsymbol{\chi}^{kl}) = \delta_{pk}\delta_{ql}$ and $e_{pq(y)}(\boldsymbol{\varphi}) = \beta_{pq}(\boldsymbol{\sigma})$, respectively. This is because the compatibility condition of strain (rate) does not allow the components of $e_{ij(y)}(\boldsymbol{v})$ to distribute arbitrarily in Y while $v_i(\boldsymbol{y}, t)$ can be an arbitrary velocity field satisfying the Y-periodicity.

2.3. Micro-stress evolution equation and macroscopic constitutive relation

Substitution of eqns (6) and (14) into eqn (2) gives an evolution equation of micro-stress such as

$$\dot{\sigma}_{ij}(\boldsymbol{y}, t) = a_{ijkl}(\boldsymbol{y})\dot{E}_{kl}(t) - r_{ij}(\boldsymbol{y}, t), \tag{15}$$

where

$$a_{ijkl} = c_{ijpq}[\delta_{pk}\delta_{ql} - e_{pq(y)}(\boldsymbol{\chi}^{kl})], \tag{16}$$

$$r_{ij} = c_{ijkl}[\beta_{kl}(\boldsymbol{\sigma}) - e_{kl(y)}(\boldsymbol{\varphi})]. \tag{17}$$

Here and from now on δ_{ij} indicates Kronecker's delta.

Now let us introduce a volume average operator

$$\langle \# \rangle = \frac{1}{|Y|}\int_Y \# \,\mathrm{d}Y, \tag{18}$$

where $|Y|$ denotes the volume of the unit cell Y. Then eqn (15) becomes a rate-type macroscopic constitutive equation

$$\dot{\Sigma}_{ij} = \langle a_{ijkl} \rangle \dot{E}_{kl} - \langle r_{ij} \rangle, \tag{19}$$

where $\dot{\Sigma}_{ij}$ indicates the macro-stress rate defined as

$$\dot{\Sigma}_{ij} = \langle \dot{\sigma}_{ij} \rangle. \tag{20}$$

Moreover, taking the volume average of eqn (6) and using the divergence theorem and the Y-periodicity of $\dot{u}_i^1$, we have

$$\dot{E}_{ij} = \langle \dot{e}_{ij} \rangle. \tag{21}$$

Then, the solution (14), the microscopic stress evolution equation (15) and the rate-type macroscopic constitutive relation (19), in combination with eqns (12) and (13) to determine the Y-periodic functions χ_i^{kl} and φ_i, enable us to find $\dot{u}_i^1(\boldsymbol{y}, t)$, $\dot{\sigma}_{ij}(\boldsymbol{y}, t)$ and either $\dot{\Sigma}_{ij}(t)$ or $\dot{E}_{ij}(t)$ if $\sigma_{ij}(\boldsymbol{y}, t)$, is known and either $\dot{E}_{ij}(t)$ or $\dot{\Sigma}_{ij}(t)$ is given. Consequently, the homogenized deformation behavior of Ω subjected to a prescribed history of either $E_{ij}(t)$ or $\Sigma_{ij}(t)$ can be computed incrementally, as will be described in detail in Section 4.

Before moving on to the next section, let us interpret the resulting equations physically. Equation (2) allows the constituents to deform elastically when strain changes very quickly. This means that the first terms in the right-hand-sides in eqns (14), (15) and (19) represent the elastic changes of u_i^1, σ_{ij} and Σ_{ij}, respectively, whereas the second terms in them are regarded as expressing the effects of viscosity. Especially $\langle a_{ijkl} \rangle$ and $\langle r_{ij} \rangle$ in eqn (19) are interpreted as the macroscopic elastic stiffness matrix and the macroscopic stress relaxation rate under constant macro-strain, respectively.

3. Homogenization based on asymptotic expansion

The homogenization problem dealt with in the macroscopically uniform case in the preceding section is discussed here more generally on the basis of the two-scale asymptotic expansion method (Bensoussan et al., 1978; Sanchez-Palencia, 1980; Bakhvalov and Panasenko, 1989; Kalamkarov, 1992). In this section, we consider an incremental formulation, in which the constitutive relation (2) is expressed as

$$\Delta\sigma_{ij} = c_{ijkl}[\Delta e_{kl} - \beta_{kl}(\boldsymbol{\sigma}_{t+\Theta\Delta t})\Delta t], \tag{22}$$

where Δ indicates increments in a time step from t to $t+\Delta t$, $\boldsymbol{\sigma}_{t+\Theta\Delta t}$ denotes the stress at $t+\Theta\Delta t$, and $0 \leqslant \Theta \leqslant 1$.

3.1. Global and local coordinates

A body Ω with a periodic internal structure is now subjected to prescribed traction $\bar{T}_i$ on a part of the boundary, Γ_T, and prescribed displacement $\bar{u}_i$ on the other part Γ_u, as shown in Fig. 2. Let

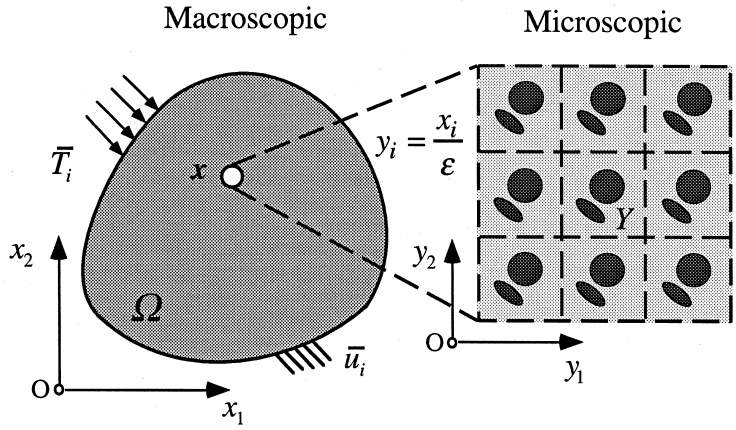

Fig. 2. Global and local problems with two spatial scales.

x_i ($i = 1, 2, 3$) be the global rectangular coordinates to analyze the macroscopic behavior of Ω, and let us suppose that the size l of the unit cell Y is much smaller than the size L of Ω:

$$\varepsilon = \frac{l}{L} \ll 1. \tag{23}$$

Then, the field variables such as stress and strain can vary rapidly in the small scale l and slowly in the large scale L. In order to represent such rapid variations explicitly, the asymptotic expansion method introduces the local coordinates y_i as

$$y_i = \frac{x_i}{\varepsilon}. \tag{24}$$

Consequently, the unit cell Y is magnified to have the same size as Ω. It is then convenient to employ the global and local coordinates, x_i and y_i, for representing the slow and rapid variations taking place macroscopically in Ω and microscopically in Y, respectively. Thus, stress, strain and displacement are expressed as $\sigma_{ij}(\boldsymbol{x}, \boldsymbol{y}, t)$, $e_{ij}(\boldsymbol{x}, \boldsymbol{y}, t)$ and $u_i(\boldsymbol{x}, \boldsymbol{y}, t)$.

When y_i is employed in addition to x_i, we have the chain rule for spatial gradient, $\mathrm{d}/\mathrm{d}\boldsymbol{x} = \partial/\partial\boldsymbol{x} + \varepsilon^{-1}\partial/\partial\boldsymbol{y}$, so that the equilibrium equation of stress increments and the relation between strain and displacement increments take forms

$$\frac{\partial \Delta\sigma_{ij}}{\partial x_j} + \frac{1}{\varepsilon}\frac{\partial \Delta\sigma_{ij}}{\partial y_j} = 0, \tag{25}$$

$$\Delta e_{ij} = e_{ij(x)}(\Delta\boldsymbol{u}) + \frac{1}{\varepsilon} e_{ij(y)}(\Delta\boldsymbol{u}). \tag{26}$$

3.2. Asymptotic expansion

The two-scale asymptotic expansion provides displacement increment Δu_i with the expression

$$\Delta u_i(\boldsymbol{x}, \boldsymbol{y}, t) = \Delta u_i^0(\boldsymbol{x}, t) + \varepsilon \Delta u_i^1(\boldsymbol{x}, \boldsymbol{y}, t) + \varepsilon^2 \Delta u_i^2(\boldsymbol{x}, \boldsymbol{y}, t) + \cdots, \tag{27}$$

where Δu_i^0 represents macroscopic displacement increment, and Δu_i^1, Δu_i^2, etc. are local perturbations satisfying the Y-periodic condition. Then substitution of eqn (27) into (26) gives

$$\Delta e_{ij} = e_{ij(x)}(\Delta\boldsymbol{u}^0) + e_{ij(y)}(\Delta\boldsymbol{u}^1) + \varepsilon[e_{ij(x)}(\Delta\boldsymbol{u}^1) + e_{ij(y)}(\Delta\boldsymbol{u}^2)] + \cdots. \tag{28}$$

Comparison of eqns (6) and (28) shows that the first two terms in the right-hand-side in eqn (28) are material in the macroscopically uniform case; in other words, the terms of order ε, ε^2 and so on arise from the nonuniformity of macroscopic deformation. It is then suggested that stress increment can be asymptotically expanded similarly to eqn (28):

$$\Delta\sigma_{ij}(\boldsymbol{x}, \boldsymbol{y}, t) = \Delta\sigma_{ij}^1(\boldsymbol{x}, \boldsymbol{y}, t) + \varepsilon \Delta\sigma_{ij}^2(\boldsymbol{x}, \boldsymbol{y}, t) + \cdots, \tag{29}$$

where the first term in the right-hand-side remains as micro-stress increment in the macroscopically uniform case.

Then, substituting eqn (29) into the incremental constitutive relation (22), we have

$$\Delta\sigma_{ij}^1+\varepsilon\Delta\sigma_{ij}^2+\cdots = c_{ijkl}[\Delta e_{kl}-\beta_{kl}(\boldsymbol{\sigma}_{t+\Theta\Delta t})\Delta t], \tag{30}$$

where

$$\beta_{kl}(\boldsymbol{\sigma}_{t+\Theta\Delta t}) = \beta_{kl}(\boldsymbol{\sigma}_t^1)+G_{klrs}(\boldsymbol{\sigma}_t^1)[\Theta\Delta\sigma_{rs}^1+\varepsilon(\sigma_{rs}^2+\Theta\Delta\sigma_{rs}^2)+\cdots], \tag{31}$$

$$G_{klrs}(\boldsymbol{\sigma}) = \frac{\partial\beta_{kl}(\boldsymbol{\sigma})}{\partial\sigma_{rs}}. \tag{32}$$

Substituting further eqn (28) into eqn (30), and collecting terms of the same order with respect to ε, we obtain

$$\Delta\sigma_{ij}^1 = \tilde{c}_{ijkl}[e_{kl(x)}(\Delta\boldsymbol{u}^0)+e_{kl(y)}(\Delta\boldsymbol{u}^1)-\beta_{kl}(\boldsymbol{\sigma}_t^1)\Delta t], \tag{33}$$

$$\Delta\sigma_{ij}^2 = \tilde{c}_{ijkl}[e_{kl(x)}(\Delta\boldsymbol{u}^1)+e_{kl(y)}(\Delta\boldsymbol{u}^2)-G_{klrs}(\boldsymbol{\sigma}_t^1)\sigma_{rs}^2\Delta t], \tag{34}$$

where

$$\tilde{c}_{ijkl} = [[c_{ijkl}]^{-1}+\Theta G_{ijkl}(\boldsymbol{\sigma}_t^1)\Delta t]^{-1}. \tag{35}$$

Moreover, use of eqn (29) changes eqn (25) into

$$\frac{1}{\varepsilon}\frac{\partial\Delta\sigma_{ij}^1}{\partial y_j}+\left(\frac{\partial\Delta\sigma_{ij}^1}{\partial x_j}+\frac{\partial\Delta\sigma_{ij}^2}{\partial y_j}\right)+\cdots = 0. \tag{36}$$

Hence it is seen that stress increments $\Delta\sigma_{ij}^1$ and $\Delta\sigma_{ij}^2$ satisfy

$$\frac{\partial\Delta\sigma_{ij}^1}{\partial y_j} = 0, \tag{37}$$

$$\frac{\partial\Delta\sigma_{ij}^1}{\partial x_j}+\frac{\partial\Delta\sigma_{ij}^2}{\partial y_j} = 0. \tag{38}$$

3.3. Microscopic and macroscopic equations

Equations (33) and (37), which were obtained from the leading order terms in eqns (30) and (36), are nothing but eqns (1) and (2) with eqn (6), which were employed as the basic equations in the macroscopically uniform case. Therefore, in the same way as in the preceding section, it can be shown that eqns (33) and (37) are combined and transformed to

$$\int_Y \tilde{c}_{ijpq}e_{pq(y)}(\Delta\boldsymbol{u}^1)e_{ij(y)}(\boldsymbol{v})\,\mathrm{d}Y = -e_{kl(x)}(\Delta\boldsymbol{u}^0)\int_Y \tilde{c}_{ijkl}e_{ij(y)}(\boldsymbol{v})\,\mathrm{d}Y+\Delta t\int_Y \tilde{c}_{ijkl}\beta_{kl}(\boldsymbol{\sigma}_t^1)e_{ij(y)}(\boldsymbol{v})\,\mathrm{d}Y, \tag{39}$$

where $v_i(\boldsymbol{x},\boldsymbol{y},t)$ is an arbitrary, Y-periodic velocity field defined in each Y at $\boldsymbol{x}$ and t. Let $\tilde{\chi}_i^{kl}$ and $\tilde{\varphi}_i$ be the functions determined, respectively, by solving

$$\int_Y \tilde{c}_{ijpq}e_{pq(y)}(\tilde{\boldsymbol{\chi}}^{kl})e_{ij(y)}(\boldsymbol{v})\,\mathrm{d}Y = \int_Y \tilde{c}_{ijkl}e_{ij(y)}(\boldsymbol{v})\,\mathrm{d}Y \quad \text{with } Y\text{-periodicity of } \tilde{\chi}_i^{kl}, \tag{40}$$

$$\int_Y \tilde{c}_{ijpq} e_{pq(y)}(\tilde{\boldsymbol{\varphi}}) e_{ij(y)}(\boldsymbol{v})\,\mathrm{d}Y = \int_Y \tilde{c}_{ijkl}\beta_{kl}(\boldsymbol{\sigma}_t^1) e_{ij(y)}(\boldsymbol{v})\,\mathrm{d}Y \quad \text{with } Y\text{-periodicity of } \tilde{\varphi}_i, \tag{41}$$

where $v_i(\boldsymbol{x}, \boldsymbol{y}, t)$ is any Y-periodic velocity field in each Y at $\boldsymbol{x}$ and t. Then eqn (39) has the following solution similar to eqn (14):

$$\Delta u_i^1(\boldsymbol{x}, \boldsymbol{y}, t) = -\tilde{\chi}_i^{kl}(\boldsymbol{x}, \boldsymbol{y}, t) e_{kl(x)}(\Delta \boldsymbol{u}^0(\boldsymbol{x}, t)) + \tilde{\varphi}_i(\boldsymbol{x}, \boldsymbol{y}, t)\Delta t. \tag{42}$$

It is noticed that not only $\tilde{\varphi}_i$ but also $\tilde{\chi}_i^{kl}$ are functions of x_j, y_j and t because in eqns (40) and (41) $\tilde{c}_{ijpq}$ depends on $\sigma_t^1(\boldsymbol{x}, \boldsymbol{y}, t)$ as expressed in eqn (35).

Then, substitution of eqn (42) into eqn (33) gives an incremental evolution equation of σ_{ij}^1,

$$\Delta\sigma_{ij}^1 = \tilde{a}_{ijkl} e_{kl(x)}(\Delta \boldsymbol{u}^0) - \tilde{r}_{ij}\Delta t, \tag{43}$$

where

$$\tilde{a}_{ijkl} = \tilde{c}_{ijpq}[\delta_{pk}\delta_{ql} - e_{pq(y)}(\tilde{\boldsymbol{\chi}}^{kl})], \tag{44}$$

$$\tilde{r}_{ij} = \tilde{c}_{ijkl}[\beta_{kl}(\boldsymbol{\sigma}_t^1) - e_{kl(y)}(\tilde{\boldsymbol{\varphi}})]. \tag{45}$$

Using the volume average operator (18), eqn (43) is transformed into a macroscopic constitutive relation

$$\Delta\Sigma_{ij} = \langle \tilde{a}_{ijkl} \rangle \Delta E_{kl} - \langle \tilde{r}_{ij} \rangle \Delta t, \tag{46}$$

where $\Delta\Sigma_{ij}$ and ΔE_{kl} are defined as

$$\Delta\Sigma_{ij} = \langle \Delta\sigma_{ij}^1 \rangle, \tag{47}$$

$$\Delta E_{kl} = e_{kl(x)}(\Delta \boldsymbol{u}^0). \tag{48}$$

The resulting equations above enable us to analyze incrementally the homogenized behavior in time-dependent deformation of Ω, as will be described in detail in Section 4. It is noticed that $\Delta\Sigma_{ij}$ defined by eqn (47) satisfies the equilibrium equation in the macroscopic scale; i.e., taking the volume average of eqn (38) in Y and using the Y-periodicity of $\Delta\sigma_{ij}^2$, we find that

$$\frac{\partial \Delta\Sigma_{ij}}{\partial x_j} = 0. \tag{49}$$

4. Computational procedure

The time-dependent behavior of nonlinear composites with periodic internal structures can be computed incrementally using eqns (40)–(48), which replace the corresponding equations in Section 2 if eqn (22) is employed instead of eqn (2) there. This section is devoted to the procedure of such computation, though only the macroscopically uniform case to evaluate the homogenized constitutive relation is considered here. The procedure needs eqns (40) and (41) to be solved for finding the Y-periodic functions $\tilde{\chi}_p^{kl}$ and $\tilde{\varphi}_k$ at the beginning in each time step. These equations can be solved numerically by means of a finite element method in which the Y-periodicity is imposed on $\tilde{\chi}_p^{kl}$ and $\tilde{\varphi}_k$ using the penalty method (see Appendix A).

Let us suppose that the unit cell Y to be analyzed is divided into finite elements with integration points, that micro-stress at current time t, $\boldsymbol{\sigma}_t^1$, is known at the integration points, and that the history of either macro-stress Σ_{ij} or macro-strain E_{ij}, or a combination of them, is prescribed. Then, the incremental computation from the current time t to the subsequent time $t+\Delta t$ can be done as follows:

(1) Calculating $\tilde{c}_{ijpq}$ and $\beta_{kl}(\boldsymbol{\sigma}_t^1)$ at the integration points in Y, and solving eqns (40) and (41), we determine the Y-periodic functions $\tilde{\chi}_i^{kl}$ and $\tilde{\varphi}_i$.
(2) We calculate $\tilde{a}_{ijkl}$ and $\tilde{r}_{ij}$ at the integration points using eqns (44) and (45), and then we average them in Y to obtain $\langle\tilde{a}_{ijkl}\rangle$ and $\langle\tilde{r}_{ij}\rangle$.
(3) Using eqn (46) with prescribed components of ΔE_{ij} and $\Delta\Sigma_{ij}$, we determine unprescribed components of ΔE_{ij} and $\Delta\Sigma_{ij}$.
(4) We calculate micro-stress increment $\Delta\sigma_{ij}^1$ using eqns (43) and (48).
(5) Adding the increments to the current values, we proceed to the next time step.

5. Examples of numerical analysis

As an application of the present theory, transverse creep of metal matrix composites reinforced unidirectionally with continuous fibers was analyzed numerically to discuss the effect of fiber arrangement on the anisotropy in the macroscopic creep behavior. It seems that such an effect has not been analyzed yet with respect to creep and plasticity.

5.1. *Fiber arrangement, material properties and loading condition*

Two types of fiber arrangement, i.e., square and hexagonal arrays were considered for the composites analyzed in this work (Fig. 3). It was assumed that the composites were under the plane-strain condition in the fiber direction and subjected to transverse macro-stress such as

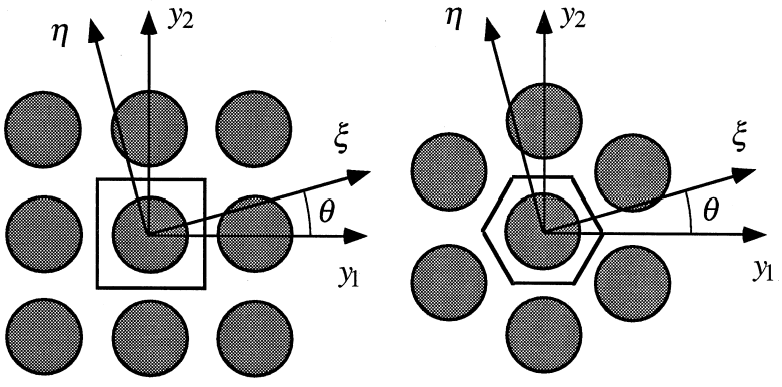

Fig. 3. Unit cell and loading direction; (a) square array, (b) hexagonal array.

$$\Sigma_{\xi\xi} = \text{constant}, \quad \Sigma_{\xi\eta} = \Sigma_{\eta\eta} = 0, \tag{50}$$

where ξ and η denote the loading coordinate axes making an angle θ with the material coordinate axes y_1 and y_2 (Fig. 3).

The fibers were assumed to obey Hooke's law

$$e_{ij} = \frac{1+\nu_f}{E_f}\sigma_{ij} - \frac{\nu_f}{E_f}\sigma_{kk}\delta_{ij}, \tag{51}$$

where ν_f and E_f are material constants. The matrix, on the other hand, was assumed to exhibit power-law creep in addition to linear elasticity, i.e.,

$$\dot{e}_{ij} = \frac{1+\nu_m}{E_m}\dot{\sigma}_{ij} - \frac{\nu_m}{E_m}\dot{\sigma}_{kk}\delta_{ij} + \frac{3}{2}A\sigma_{eq}^{n-1}s_{ij}, \tag{52}$$

where ν_m, E_m, A and n are material constants, s_{ij} indicates the deviatoric part of micro-stress σ_{ij}, and $\sigma_{eq} = [(3/2)s_{ij}s_{ij}]^{1/2}$.

For convenience in computation, the following nondimensional stresses, strains and time were introduced:

$$\sigma_{ij}^* = \frac{\sigma_{ij}}{\sigma_0}, \quad \Sigma_{ij}^* = \frac{\Sigma_{ij}}{\sigma_0}, \quad e_{ij}^* = \frac{E_f e_{ij}}{\sigma_0}, \quad E_{ij}^* = \frac{E_f E_{ij}}{\sigma_0}, \quad t^* = AE_f\sigma_0^{n-1}t, \tag{53}$$

where σ_0 indicates an appropriate reference stress. Equations (51) and (52) were then non-dimensionalized as

$$e_{ij}^* = (1+\nu_f)\sigma_{ij}^* - \nu_f\sigma_{kk}^*\delta_{ij}, \tag{54}$$

$$\frac{\partial e_{ij}^*}{\partial t^*} = \frac{E_f}{E_m}\left[(1+\nu_m)\frac{\partial\sigma_{ij}^*}{\partial t^*} - \nu_m\frac{\partial\sigma_{kk}^*}{\partial t^*}\delta_{ij}\right] + \frac{3}{2}(\sigma_{eq}^*)^{n-1}s_{ij}^*, \tag{55}$$

where s_{ij}^* indicates the deviatoric part of σ_{ij}^* and $\sigma_{eq}^* = [(3/2)s_{ij}^*s_{ij}^*]^{1/2}$. Consequently the material parameters to be specified in computation were E_f/E_m, ν_f, ν_m and n in addition to the fiber volume fraction V_f. By supposing a titanium alloy reinforced with continuous SiC fibers (Kroupa and Neu, 1994), they were chosen as

$$\frac{E_f}{E_m} = 4, \quad \nu_f = 0.25, \quad \nu_m = 0.34, \quad n = 4, \quad V_f = 0.395. \tag{56}$$

A 2-D finite element program was developed to solve eqns (40) and (41) and to perform the computational procedure described in Section 4. In the program, four node isoparametric elements with 2×2 Gaussian integration points were used, and the penalty method was utilized to impose the Y-periodic boundary condition on $\tilde{\chi}_p^{kl}$ and $\tilde{\varphi}_k$ (Appendix A). Figures 4(a) and (b) show the unit cells and finite element meshes used for the square and hexagonal arrays in this work, respectively.

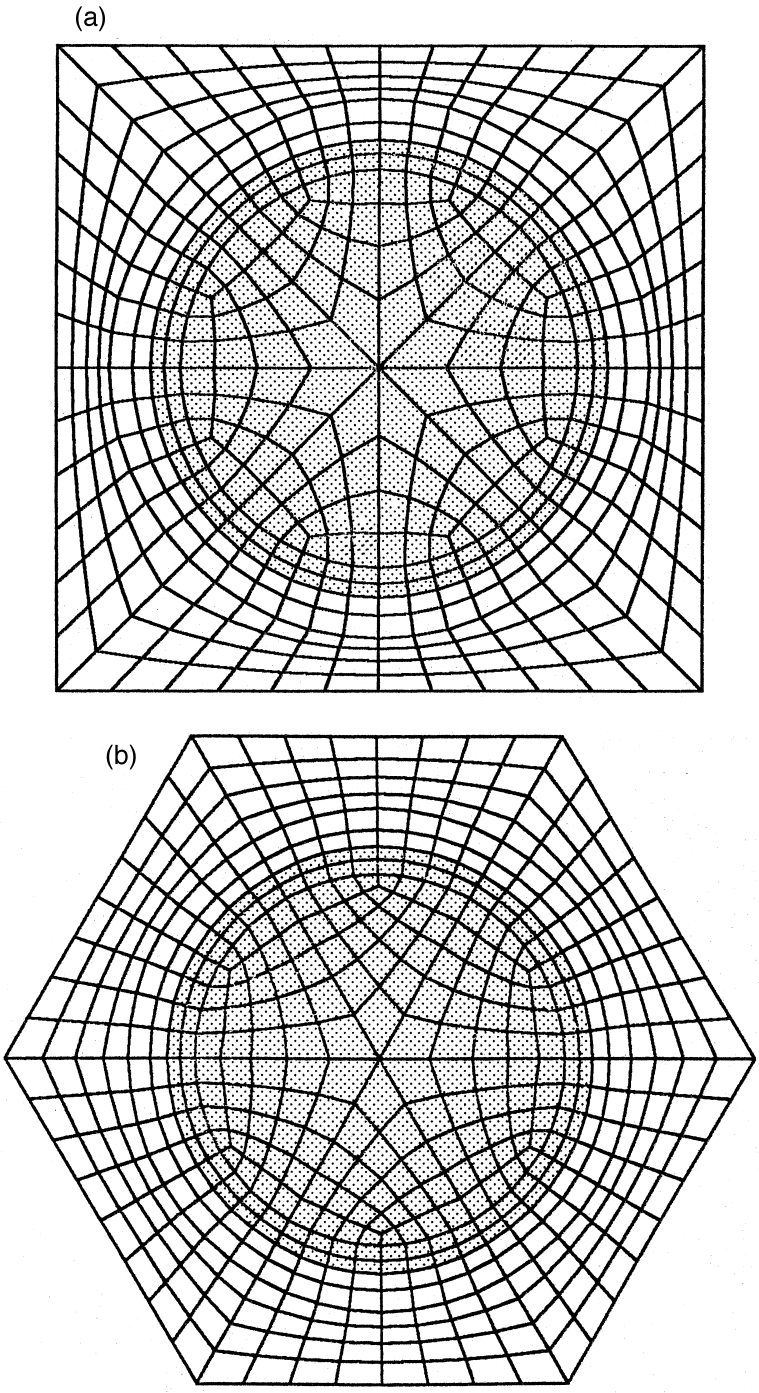

Fig. 4. Finite element mesh; (a) square array, (b) hexagonal array.

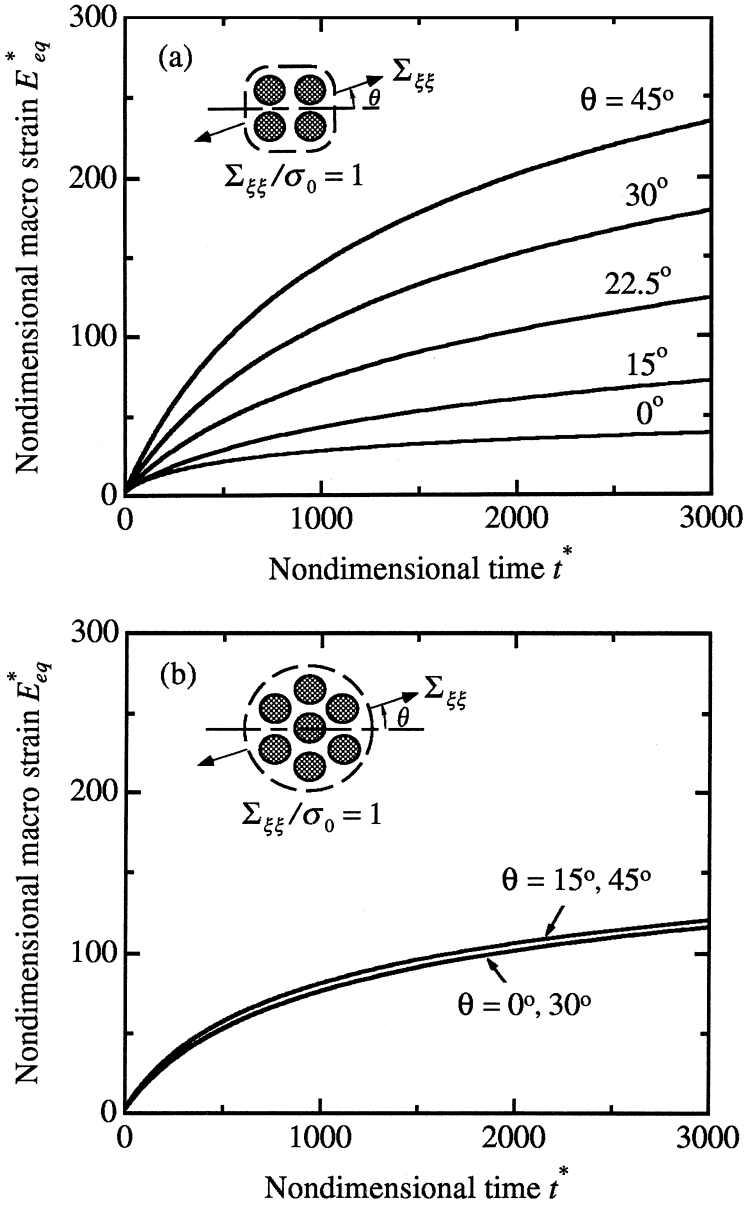

Fig. 5. Changes of equivalent macro-strain with time in tensile creep at $\Sigma^*_{\xi\xi} = 1$ under plane strain condition; (a) square array, (b) hexagonal array.

5.2. *Results of numerical analysis*

The time-dependent changes of macro-strain for the square and hexagonal arrays are shown in Figs 5(a) and (b), respectively, the ordinates of which are taken to be the nondimensional equivalent strain defined as

$$E^*_{eq} = (\tfrac{2}{3} E^*_{ij} E^*_{ij})^{1/2}. \tag{57}$$

It is seen from Figs 5(a) and (b) that the square and hexagonal arrays exhibit significant and negligible anisotropy in transverse creep, respectively. For the square array, strain for $\theta = 45^\circ$ is about six times larger than that for $\theta = 0^\circ$ (Fig. 5(a)). This difference is very large, but it is noticed that the difference is only 11% with respect to elastic strain at $t = 0$. Hence we can say that the nonlinearity in creep magnifies outstandingly the transverse anisotropy in the case of the square array. For the hexagonal array, on the other hand, the creep curves calculated for $\theta = 0^\circ$ and $\theta = 30^\circ$ are almost the same, so that the creep behavior is nearly isotropic (Fig. 5(b)). It can be proved that the homogenized behavior in transverse creep of hexagonally fiber-arrayed composites is invariant under the 30° rotation of the loading direction if the effect of hydrostatic stress is macroscopically negligible (Appendix B); of course, the material symmetry in the hexagonal array allows it to be invariant under the 60° rotation of the loading direction. Incidentally, the hexagonal symmetry makes the elastic behavior transversely isotropic macroscopically, which is similar to the in-plane quasi isotropy in laminated plates of $0^\circ/\pm 60^\circ$ (Christensen, 1979).

It is also seen from Figs 5(a) and (b) that transient creep takes place very noticeably, and that transient creep strain becomes much larger before reaching the steady state than initial elastic strain. This suggests that it is not sufficient to analyze only the steady state in creep, and that the analysis of transient creep as in the present work is important. Let us point out that the transient creep in the figures is entirely due to the load transfer from the matrix to the fibers because any strain hardening of the matrix is not taken into account in eqn (52).

Figure 6 shows the relations between the maximum principal directions of macro-stress and macro-strain rate, Φ_Σ and $\Phi_{\dot{E}}$, at the nondimensional time of $t^* = 1500$ obtained in the present analysis of tensile creep. Here Φ_Σ and $\Phi_{\dot{E}}$ indicate the angles which the maximum principal directions make with the y_1-axis. It is seen from the figure that the data for the square array, except for $\theta = 0^\circ$ and $\theta = 45^\circ$, deviate from the line of $\Phi_\Sigma = \Phi_{\dot{E}}$ whereas the data for the hexagonal array lie almost completely on the line. Since the line indicates transverse isotropy, the relations between Φ_Σ and $\Phi_{\dot{E}}$ in Fig. 6 also confirm that the square and hexagonal arrays exhibit significant and negligible anisotropy in transverse creep, respectively.

Finally we are concerned with the microscopic state of deformation in the unit cells. Figures 7(a)–(d) show the deformed meshes of the unit cells at $t^* = 1500$ in the two representative cases of $\theta = 0^\circ$ and $\theta = 45^\circ$. As seen from the figures, the matrix exhibits significant deformation due to creep, which is in contrast to little elastic deformation in the fibers. This suggests that macroscopic deformation proceeds almost incompressibly with time for both the square and hexagonal arrays. It is also seen from the figures that some finite elements in the matrix near the fiber/matrix interface are deformed noticeably by shear resulting from the difference of rigidity between the matrix and the fibers. Figures 8(a)–(d) depict the distributions of microscopic creep strain at $t^* = 1500$ with respect to the equivalent value $e^{c^*}_{eq}$, which is defined in terms of the creep component $e^{c^*}_{ij}$ of nondimensional micro-strain e^*_{ij} as $e^{c^*}_{eq} = [(2/3)e^{c^*}_{ij} e^{c^*}_{ij}]^{1/2}$. For the square array, creep strain concentrates near the fiber in the case of $\theta = 0^\circ$ whereas in the case of $\theta = 45^\circ$ it takes place markedly even near the cell corners (Figs 8(a) and (b)). This difference accounts for small and large values of macroscopic creep strain in the two cases shown in Fig. 5(a). For the hexagonal array, on the other hand, creep strain distributes fairly broadly in the matrix, as shown in Figs 8(c) and (d), where it is noticed that the two cases of $\theta = 0^\circ$ and $\theta = 45^\circ$ have considerably different distributions of microscopic creep strain in spite of nearly the same macroscopic creep curves in Fig. 5(b).

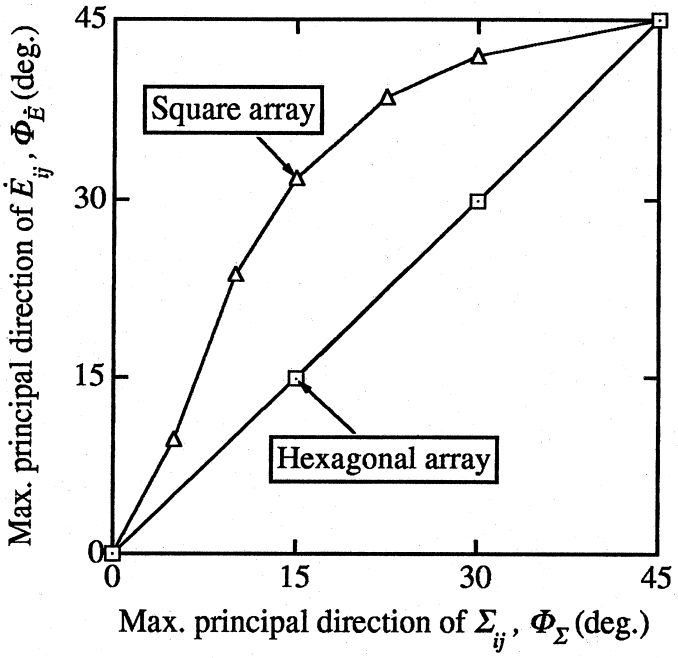

Fig. 6. Relation between the maximum principal direction of macro-stress, Φ_{Σ}, and that of macro-strain rate, $\Phi_{\dot{E}}$ at $t^* = 1500$ in tensile creep at $\Sigma^*_{\xi\xi} = 1$ under plane strain condition; Φ_{Σ} and $\Phi_{\dot{E}}$ are the angles measured from the y_1-axis.

6. Conclusions

A homogenization theory for time-dependent deformation such as creep and viscoplasticity of nonlinear composites with periodic internal structures was described within the framework of infinitesimal strain. The theory was developed first in the macroscopically uniform case in a rate form without recourse to the asymptotic expansion of field variables, and then it was extended to the macroscopically nonuniform case in an incremental form using the asymptotic expansion. Thus a homogenized constitutive equation and a microscopic stress evolution equation were derived in rate and incremental forms by defining two kinds of Y-periodic functions determined by solving two unit cell problems. Then it was shown that the theory enables us to compute incrementally the time-dependent deformation behavior by discretizing unit cells with finite elements, and that the theory is effective for problems in which the history of either macro-stress or macro-strain, or a combination of them, is prescribed. As an application of the theory, transverse creep of metal matrix composites reinforced unidirectionally with continuous fibers was analyzed for square and hexagonal fiber arrays. Consequently it was found that the square and hexagonal arrays exhibit significant and negligible anisotropy in the transverse creep, respectively.

Let us emphasize that the rate and incremental approaches employed in the present work for time-dependent nonlinear composites were not taken in the previous works on homogenization for linear viscoelastic composites by Sanchez-Palencia (1980), Francfort and Suquet (1986) and Shibuya (1996).

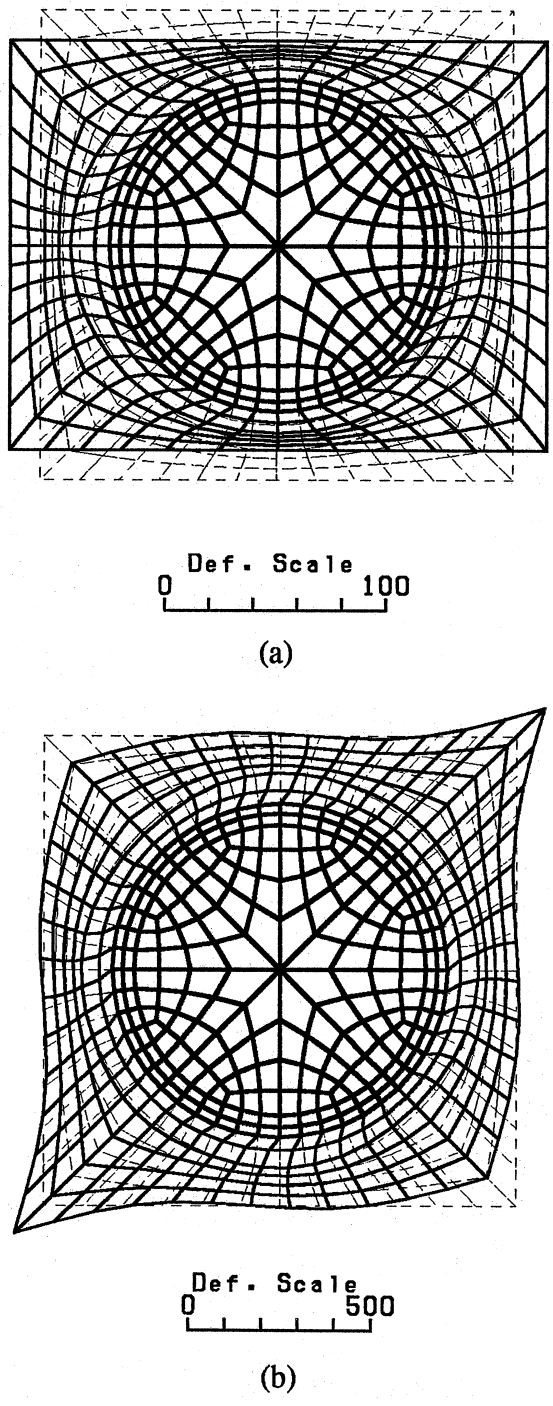

Fig. 7. Deformation of unit cell at $t^* = 1500$ in tensile creep at $\Sigma^*_{\xi\xi} = 1$ under plane strain condition; (a) square array ($\theta = 0^\circ$), (b) square array ($\theta = 45^\circ$), (c) hexagonal array ($\theta = 0^\circ$), (d) hexagonal array ($\theta = 45^\circ$).

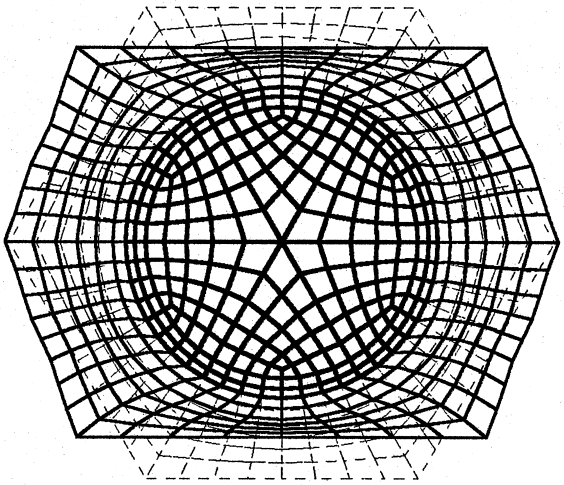

(c)

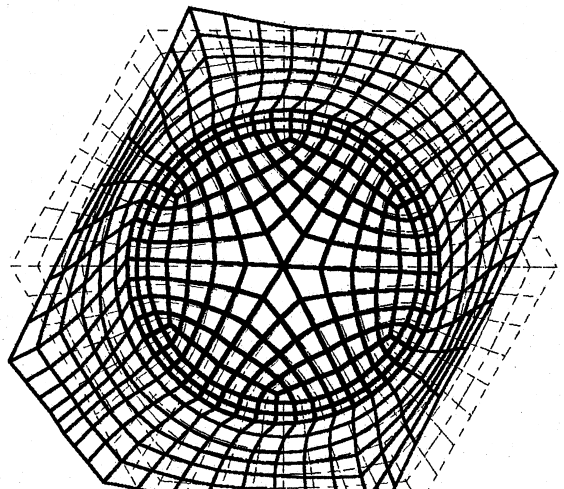

(d)

Fig. 7 (*continued*).

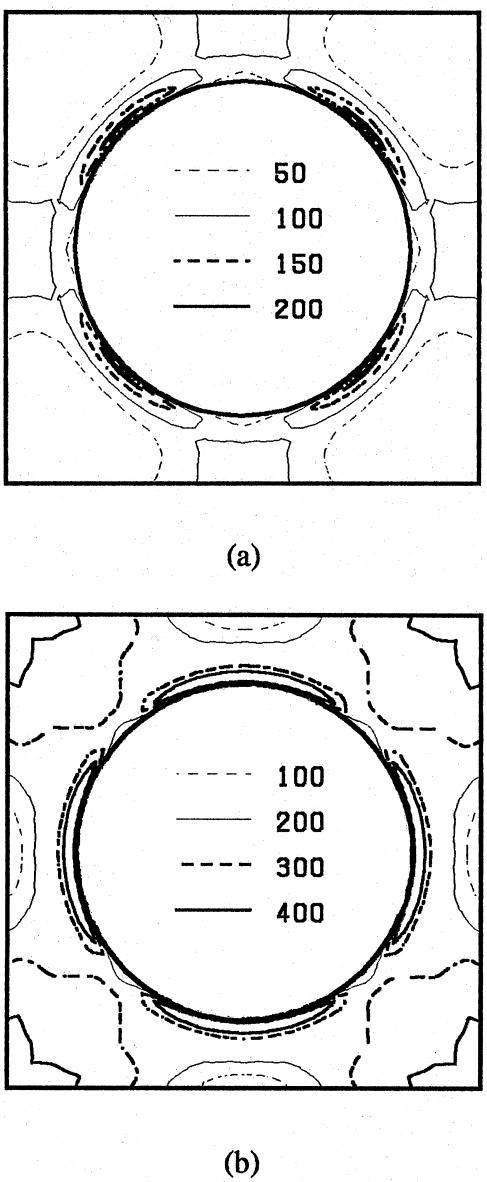

Fig. 8. Contours of equivalent micro-creep strain at $t^* = 1500$ in tensile creep at $\Sigma^*_{\xi\xi} = 1$ under plane strain condition; (a) square array ($\theta = 0^\circ$), (b) square array ($\theta = 45^\circ$), (c) hexagonal array ($\theta = 0^\circ$), (d) hexagonal array ($\theta = 45^\circ$).

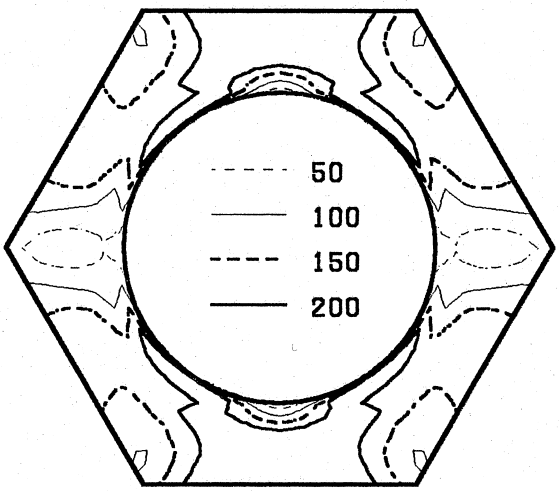

(c)

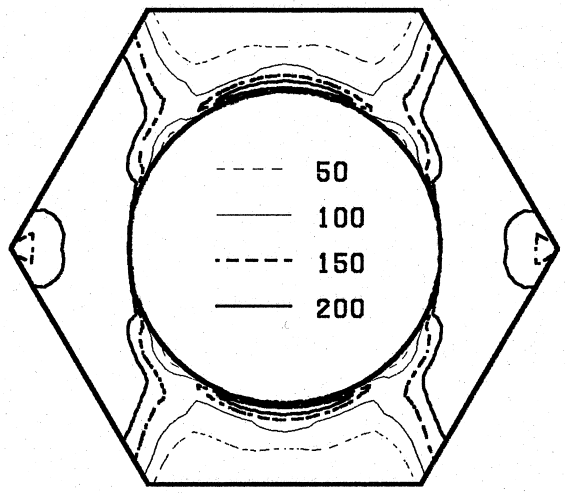

(d)

Fig. 8 (*continued*).

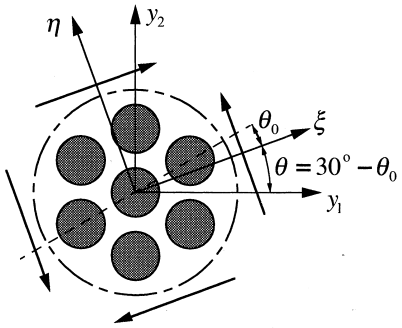

(a)

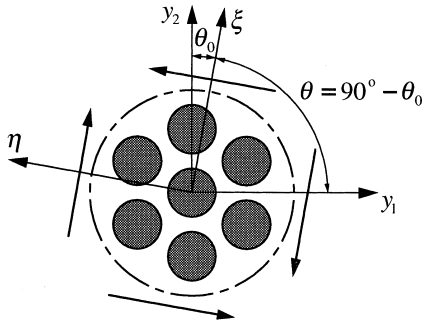

(b)

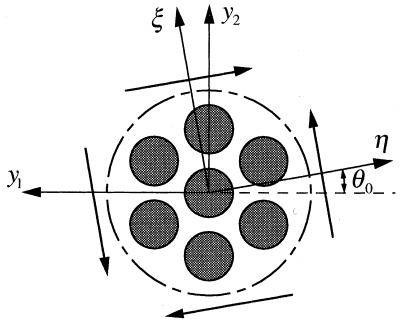

(c)

Fig. 9. Equivalence between the loading directions of $\theta = 30^\circ - \theta_0$ and $\theta = \theta_0$ under pure shear; (a) $\theta = 30^\circ - \theta_0$, (b) $\theta = 90^\circ - \theta_0$, (c) $\theta = \theta_0$.

Acknowledgements

This work was supported in part by the Ministry of Education under a Grant-in-Aid for Scientific Research B (No. 09450046). The authors are grateful to one of the reviewers for his invaluable comments related to the decomposition of microscopic displacement rate into elastic and viscous parts.

Appendix A

Equations (40) and (41) were cast into the following forms for the finite element analysis in the present work by referring to Zienkiewicz and Taylor (1987):

$$\left(\int_Y [B]^{\mathrm{T}}[\tilde{C}][B]\,\mathrm{d}Y+\lambda[L]^{\mathrm{T}}[L]\right)\{\tilde{\chi}^{kl}\} = \int_Y [B]^{\mathrm{T}}\{\tilde{C}^{kl}\}\,\mathrm{d}Y, \tag{A1}$$

$$\left(\int_Y [B]^{\mathrm{T}}[\tilde{C}][B]\,\mathrm{d}Y+\lambda[L]^{\mathrm{T}}[L]\right)\{\tilde{\varphi}\} = \int_Y [B]^{\mathrm{T}}[\tilde{C}]\{\beta\}\,\mathrm{d}Y, \tag{A2}$$

where the supposed T denotes the transpose, $[B]$ the strain matrix, $[\tilde{C}]$ the stiffness matrix representing $\tilde{c}_{ijkl}$, $\{\tilde{\chi}^{kl}\}$ and $\{\tilde{\varphi}\}$ the nodal values of $\tilde{\chi}_i^{kl}$ and $\tilde{\varphi}_i$, respectively, $\{\tilde{C}^{kl}\}$ the vector consisting of $\tilde{c}_{ijkl}$ with given k and l, $\{\beta\}$ the vector for creep rate $\beta_{ij}(\boldsymbol{\sigma}_t^1)$, λ the penalty number, and $[L]$ the constraint matrix to impose the Y-periodic condition on $\tilde{\chi}_i^{kl}$ and $\tilde{\varphi}_i$ at the boundary of Y. The nodal values of $\tilde{\chi}_i^{kl}$ and $\tilde{\varphi}_i$ were set to be zero at one corner of the boundary of Y.

Appendix B

Let us consider pure shear creep of hexagonally fiber-arrayed composites subjected to $\Sigma_{\xi\eta}$ = constant and $\Sigma_{\xi\xi} = \Sigma_{\eta\eta} = 0$ (Figs 9(a) to (c)). Then, because of the material symmetry, the pure shear creep of $\theta = 30^\circ - \theta_0$ shown in Fig. 9(a) is identical to that of $\theta = 90^\circ - \theta_0$ in Fig. 9(b), where $0 \leqslant \theta_0 \leqslant 15^\circ$. The pure shear creep of $\theta = 90^\circ - \theta_0$ is reflected with respect to the y_2-axis, resulting in the pure shear creep of $\theta = \theta_0$ shown in Fig. 9(c). In the pure shear creep, therefore, hexagonally fiber-arrayed composites exhibit the same behavior in the two loading directions of $\theta = 30^\circ - \theta_0$ and $\theta = \theta_0$.

Now we suppose that deformation is macroscopically incompressible. Then, the pure shear creep discussed above has the same principal macro-strains in ratio as the plane strain tensile creep analyzed in the present work. Consequently the proof above allows us to say that the plane strain tensile creep of hexagonally fiber-arrayed composites has macroscopically no difference between the two loading directions of $\theta = 30^\circ - \theta_0$ and $\theta = \theta_0$ if deformation is macroscopically incompressible.

References

Agah-Tehrani, A., 1990. On finite deformation of composites with periodic microstructure. Mechanics of Materials 8, 255–268.

Aravas, N., Cheng, C., Ponte Castaneda, P., 1995. Steady-state creep of fiber-reinforced composites: constitutive equations and computational issues. International Journal of Solids and Structures 32, 2219–2244.

Bakhvalov, N., Panasenko, G., 1989. Homogenization: Averaging Processes in Periodic Media. Kluwer Academic Publishers, Dordrecht, The Netherlands.

Bensoussan, A., Lions, J.L., Papanicolaou, G., 1978. Asymptotic Analysis for Periodic Structures. North-Holland, Amsterdam.

Christensen, R.M., 1979. Mechanics of Composite Materials. Wiley-Interscience, New York, pp. 153–160.

Ene, H.I., 1983. On linear thermoelasticity of composite materials. International Journal of Engineering Science 21, 443–448.

Fotiu, P.A., Nemat-Nasser, S., 1996. Overall properties of elastic–viscoplastic periodic composites. International Journal of Plasticity 12, 163–190.

Francfort, G.A., 1983. Homogenization and linear thermoelasticity. SIAM Journal on Mathematical Analysis 14, 696–708.

Francfort, G.A., Suquet, P.M., 1986. Homogenization and mechanical dissipation in thermoelasticity. Archives for Rational Mechanics and Analysis 96, 265–293.

Guedes, J.M., Kikuchi, N., 1990. Preprocessing and postprocessing for materials based on the homogenization method with adaptive finite element methods. Computer Methods in Applied Mechanics and Engineering 83, 143–198.

Hoff, N.J., 1954. Approximate analysis of structures in the presence of moderately large creep deformations. Quarterly of Applied Mathematics 12, 49–55.

Jansson, S., 1992. Homogenized nonlinear constitutive properties and local stress concentrations for composites with periodic internal structure. International Journal of Solids and Structures 29, 2181–2200.

Kalamkarov, A.L., 1992. Composite and Reinforced Elements of Construction. John Wiley and Sons, Chichester.

Kroupa, J.L., Neu, R.W., 1994. The nonisothermal viscoplastic behavior of a titanium–matrix composite. Composite Engineering 4, 965–977.

Lene, F., Leguillon, D., 1982. Homogenized constitutive law for a partially cohesive composite material. International Journal of Solids and Structures 18, 443–458.

Li, J., Weng, G.J., 1997. A secant-viscosity approach to the time-dependent creep of an elastic–viscoplastic composite. Journal of the Mechanics and Physics of Solids 45, 1069–1083.

Murakami, H., Impelluso, T.J., Hegemier, G.A., 1992. Development of a mixture model for nonlinear wave propagation in fiber-reinforced composites. International Journal of Solids and Structures 29, 1919–1937.

Murakami, H., Maewal, A., Hegemier, G.A., 1981. A mixture theory with a director for linear elastodynamics of periodically laminated media. International Journal of Solids and Structures 17, 155–173.

Sanchez-Palencia, E., 1980. Non-homogeneous Media and Vibration Theory. Lecture Notes in Physics, vol. 127. Springer-Verlag, Berlin.

Shibuya, Y., 1996. Evaluation of creep compliance of carbon-fiber-reinforced composites by homogenization theory. Transactions of the Japan Society of Mechanical Engineers, Ser. A 62, 1665–1671 (in Japanese).

Suquet, P.M., 1983. Local and global aspects in the mathematical theory of plasticity. In: Sawczuk, A., Bianchi, G. (Eds.), Plasticity Today: Modelling, Methods and Applications. Elsevier, London, pp. 279–310.

Suquet, P.M., 1985. Elements of homogenization for inelastic solid mechanics. In: Sanchez-Palencia, E., Zaoui, A. (Eds), Homogenization Techniques for Composite Media. Lecture Notes in Physics, vol. 272. Springer-Verlag, Berlin. pp. 193–278.

Takano, N., Zako, M., 1995. Nonlinear analysis of woven fabric composite materials by homogenization method considering microscopic fracture. Journal of the Society of Materials Science, Japan 44, 1231–1237 (in Japanese).

Terada, K., Yuge, K., Kikuchi, N., 1995. Elasto-plastic analysis of composite materials using the homogenization method (1st report, formulation). Transactions of the Japan Society of Mechanical Engineers, Ser. A61, 2199–2205 (in Japanese).

Zienkiewicz , O.C., Taylor, R.L., 1987. The Finite Element Method, 4th ed. McGraw-Hill, London.